

Chapter 3

Trans-Alfvenic magnetohydrodynamic turbulence in the vicinity of supernova remnant Cassiopeia-A shocks ¹

3.1 Introduction

Supernovae and their remnants are the important gradients of the ISM that affect its evolution by enriching it with high mass elements and are believed to accelerate the cosmic rays (CRs) up to knee energy ($10^{15.5}$ eV). In the diffusive shock acceleration model, the magnetic field disturbances are considered to play the primary role in the acceleration of the cosmic rays (Bell, 1978, 2004; Blandford and Ostriker, 1978). In this model, the maximum energy of the CRs is found to be dependent on their diffusion coefficient. The scattering of the CRs also depends upon the magnetic field distribution (Jokipii, 1966). If the magnetic field disturbances have the continuous magnetic energy spectrum, then the view that the CR particle may resonate with this continuous energy spectrum indicates that the maximum

¹The work presented in this chapter is derived from the original work published as "Trans-Alfvenic magnetohydrodynamic turbulence in the vicinity of supernova remnant Cassiopeia-A shocks" by Vishwakarma and Kumar (2020).

energy of the CR particle and diffusion coefficient, both are related to the magnetic field disturbances. If the power-law index of the continuous monochromatic magnetic field disturbances is m (i.e. it is $\propto x^m$), then the diffusion coefficient D of the CR particle is also supposed to be a power-law with its index $1-m$ i.e. $D(E) \propto E^{1-m}$. Here x and E are the length scale of the magnetic field disturbances and the energy of the Cosmic Ray particle (Blandford and Eichler, 1987; Parizot et al., 2006). If the above power-law index (m) is $2/3$ i.e. is of trans-Alfvénic nature of magnetohydrodynamic (MHD) turbulence as analyzed by Goldreich and Sridhar (1995), then theoretically, the maximum energy of the Cosmic Ray protons (E_{pmax}) is found to be almost the same as knee energy (under some possible models of the sock compression ratio) for the supernovae remnants Cassiopeia-A, Keplar and Tycho (Parizot et al., 2006). To validate the above theoretical predictions, we need the observational results of the magnetic energy spectrum in supernovae remnants (SNRs). The validity of the above theoretical prediction is also dependent on the shape of the magnetic energy spectrum in SNR, as it is most debated in the literature whether it is a single power-law (Goldreich and Sridhar, 1995), break power law (Brandenburg and Subramanian, 2005; Lazarian and Vishniac, 1999; Xu and Lazarian, 2016, 2017) or spectrum with several peaks (Vladimirov et al., 2009). So the natural question that arises here is: whether it is possible that these SNRs can accelerate the CR protons up to knee energy and have $2/3$ power-law index like statistics of the magnetic field disturbances? Do they have a common single power-law? Break power law? Or spectrum with several peaks? To answer such questions, we need to measure the observational magnetic energy spectrum in the SNRs. There have been efforts to quantify and to measure it with the help of the two-point correlation function of the synchrotron intensities (Akauchi et al., 2017; Chepurinov, 1999; Getmantsev, 1959; Roy et al., 2009), but these correlations are biased as they have the effect of the geometry of the source in their estimators. This effect can be avoided using a method developed by Shimoda et al. (2018), if the source of emission is

a spherical object. Using this recently developed method, here we quantify statistics of the magnetic field disturbances in the SNR Cassiopeia-A. In section 3.2, we discuss the method in short for it, while analysis is discussed in section 3.3. The measured result is presented in section 3.4, and finally, discussion on the results is presented in section 3.5.

3.2 Method

The details of the developed methodology to calculate the magnetic energy spectrum in the supernova remnants using the two-point correlation function is presented in Shimoda et al. (2018). If we represent I_ν as a synchrotron intensity per frequency, then the statistics of the magnetic energy fluctuation can be represented as

$$\begin{aligned} C_{I_\nu}^2(\delta r) &= \frac{\int I_\nu(r)I_\nu(r')d^2r}{\int d^2r} \\ &\equiv \langle I_\nu(r)I_\nu(r + \delta r) \rangle_r. \end{aligned} \quad (3.1)$$

Here $r(x,y)$ represents the locus of the two dimensional positions at the radius r from the centre of the supernova. δr represents the separation between two points on the radius r such that $r - r' = \delta r$. The subscript r in the ensemble average stands to represent that the measurement of the $C_{I_\nu}^2$ is done at radius r having width Δr such that $\Delta r \ll r$, hence the measurement of $C_{I_\nu}^2$ is almost one dimensional. If the object is of spherical shape (i.e. like spherical supernova) then $C_{I_\nu}^2$ is free from geometrical effect as the depth along the line of sight at radius r is constant. Here in our analysis we use the statistics $|C_{I_\nu}^2(\delta r) - C_{I_\nu}^2(\delta r_{min})|$ so that the fluctuating component of the magnetic field could be clarified. If this statistics follows the power law then

$$|C_{I_\nu}^2(\delta r) - C_{I_\nu}^2(\delta r_{min})| = A\delta r^\alpha \quad (3.2)$$

Here, A and α being the amplitude and the power law index respectively. The uncertainty associated with above correlation statistics $|C_{I_v}^2(\delta r) - C_{I_v}^2(\delta r_{min})|$ can be written as

$$\sigma_C = A\alpha\delta r^{\alpha-1}\sigma_{\delta r} \quad (3.3)$$

Here $\sigma_{\delta r}$ is the measured uncertainty in δr . Using the measured uncertainties σ_C and $\sigma_{\delta r}$, we estimate a rough uncertainty in the measurement of the power-law index α . Wherever required, we plot and show $|C_{I_v}^2(\delta r)/C_{I_v}^2(0) - 1|$, so that the level of the fluctuation could be easily identified as a function of the length scale. For the trans-Alfvenic magnetohydrodynamic turbulence (or Kolmogorov like), the measured value of the α should be $2/3$ within its uncertainty measurement.

3.3 Analysis

Supernova remnants Cassiopeia-A (Cas-A) is a spherical shell of radius $R \sim 5$ (Reed et al., 1995). We analyzed the continuum image of the Cassiopeia A, published by Chowdhury and Chengalur (2019). The image was produced by the observations of the Gaint Meterwave Radio Interferometer (Swarup et al., 1991) in the radio frequency band 410-450 MHz. The observation details, calibration process, and the imaging method can be seen in the Chowdhury and Chengalur (2019). Figure 3.1 shows the RMS normalized continuum image of Cas-A published in the Vishwakarma and Kumar (2020). The pixel size in this image is $1''$. To measure $C_{I_v}^2(\delta r)$ we have chosen the centre of the Cassiopeia-A as 23:23:26.10, +58:48:53.70 (J2000) which is approximately same as described radio centre of the Cassiopeia-A by Arias et al. (2018) and almost the same as reverse shock centre measured by Gotthelf et al. (2001) at 23:23:25.44,+ 58:48:52.3 (J2000). For the measurement of $C_{I_v}^2(\delta r)$, we take the width of the each radius $3''$ ($\Delta r = 3''$). In the measurement of $C_{I_v}^2(\delta r)$, we use only the pixels which satisfy the condition of $I_v > 3\sigma_{rms}$,

so that any noise statistics in the $C_{I_v}^2(\delta r)$ could be avoided. We measure the $C_{I_v}^2(\delta r)$ from the radius $0.526R$ ($78''$) to $1.093R$ ($164''$) and each radius have 3 pixels as mentioned earlier. After the measurement of $C_{I_v}^2(\delta r)$ in the above radial window, we analysed the statistics $|C_{I_v}^2(\delta r) - C_{I_v}^2(\delta r_{min})|$ and found that this have the power-law like behavior in the radial windows $0.613R$ - $0.653R$, $0.760R$ - $0.800R$ and $0.980R$ - $1.020R$. We call these regions as region 1, region 2 and region 3, respectively. In the Cassiopeia-A, there are some bright knots, which give it an access power at the lowest scale; hence statistics $|C_{I_v}^2(\delta r) - C_{I_v}^2(\delta r_{min})|$ do not have the power-law like behavior at lowest scale. Because of these bright knots, the shape of the Cassiopeia-A also seems to be a little bit deviated from the complete spherical shell, but given that this deviation is not quite large, its geometrical effect on $C_{I_v}^2(\delta r)$ is expected to be negligible. Measurements of σ_c is done from the known values of the $\sigma_{\delta r}$ using the equation 3.3 for the cases where statistics of the fluctuation is a power-law with index close to the $2/3$. First we fit the $|C_{I_v}^2(\delta r) - C_{I_v}^2(\delta r_{min})|$ and calculate a rough values of the A and α (we call it the 0^{th} order approximation). Now using this zeroth-order approximation of A and α and known values of the $\sigma_{\delta r}$ we again calculate the σ_c with the help of the same equation 3.3. We now again fit the $|C_{I_v}^2(\delta r) - C_{I_v}^2(\delta r_{min})|$ with the new estimates of the σ_c and call the fitted values of A and α as the first-order approximation values. We continue the fitting process by estimating the new values of σ_c , A , and α until we find that now there is no improvement in the values of the A and α . In our measurements, the 1st order approximation is almost stable, and higher-order approximation do not differ from it to any significant amount. We also noted that $C_{I_v}^2(\delta r)$ is almost same as $C_{I_v}^2(0)$ at each radius of measurements. To constraint the max value of the δr , we take the maximum values of the normalized statistics $|C_{I_v}^2(\delta r)/C_{I_v}^2(0) - 1|$ not exceeding 0.5, as the magnetic field at larger scales guide the magnetic field at lower scales (Cho and Vishniac, 2000a). The fitted ranges of the regions 1, 2, and 3 are found to be 8 - $65''$, 9 - $182''$ and 10 - $105''$. In the next section, we will call regions 1, 2 and 3 as the

Table 3.1 The position and width information about the different regions of the supernova used in the analysis.

region name	mean radius(r/R)	range of region (r/R)
region 1	0.633	0.613-0.653
region 2	0.780	0.760-0.800
region 3	1.000	0.980-1.020

sub-shock region (SSR), reverse shock region (RSR), and forward shock region (FSR) and will justify the reason behind it.

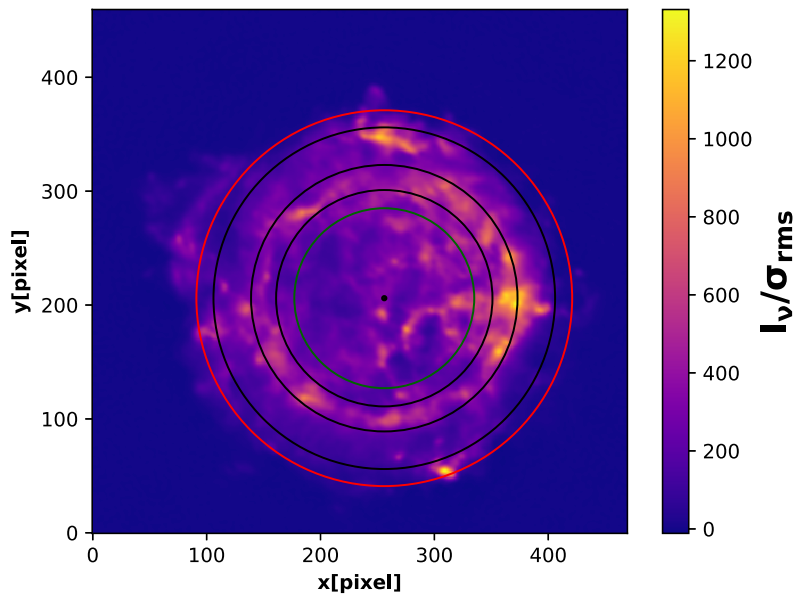


Fig. 3.1 : Continuum image of the Cas-A. Here central dot point shows the center of the SNR. The innermost and outermost circles define the region in which the correlation function is measured. The three inner consecutive black circles with mean radii at $0.633R$, $0.780R$ and $1.000R$ define the positions of the shocks and subshock in the SNR in terms of the radius R of the supernova. The exact range defining the three regions are given in table 3.1.

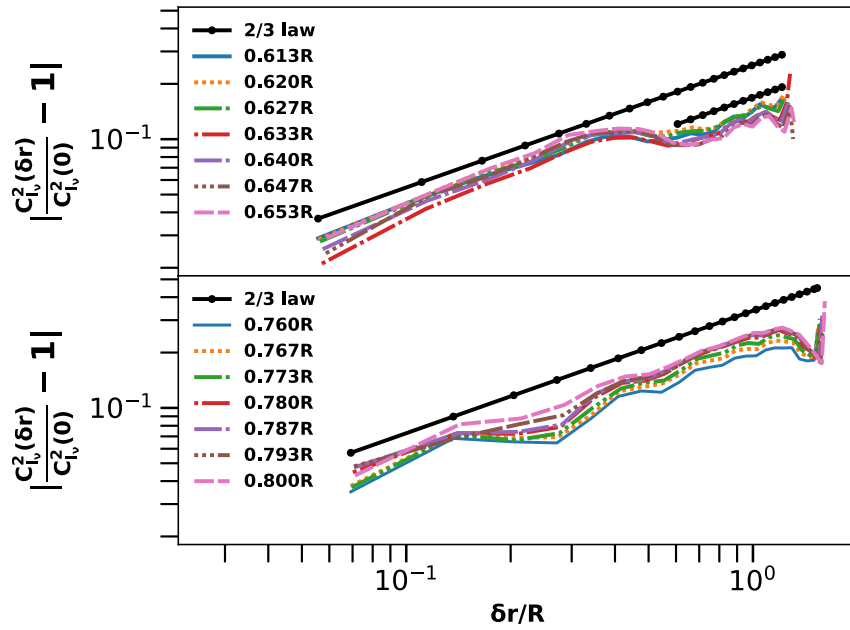


Fig. 3.2 : Spectra of region 1 (upper panel) and region 2 (lower panel). For comparison we have plotted 2/3 law point to point.

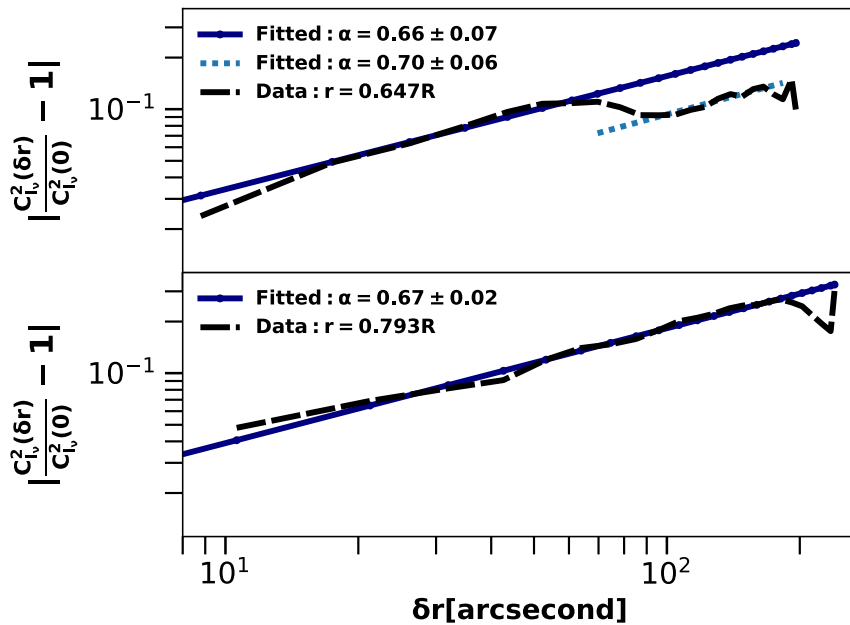


Fig. 3.3 : One of the best chosen spectra from region 1 (upper panel) and region 2 (lower panel) as shown in figure 3.2.

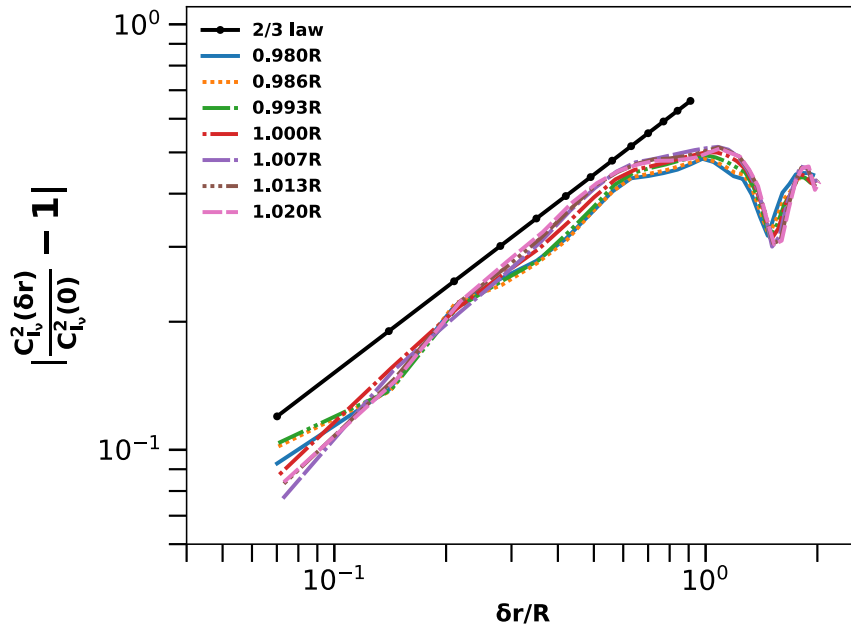


Fig. 3.4 : Spectra of region 3 showing the compatibility with 2/3 law near to the forward shock position.

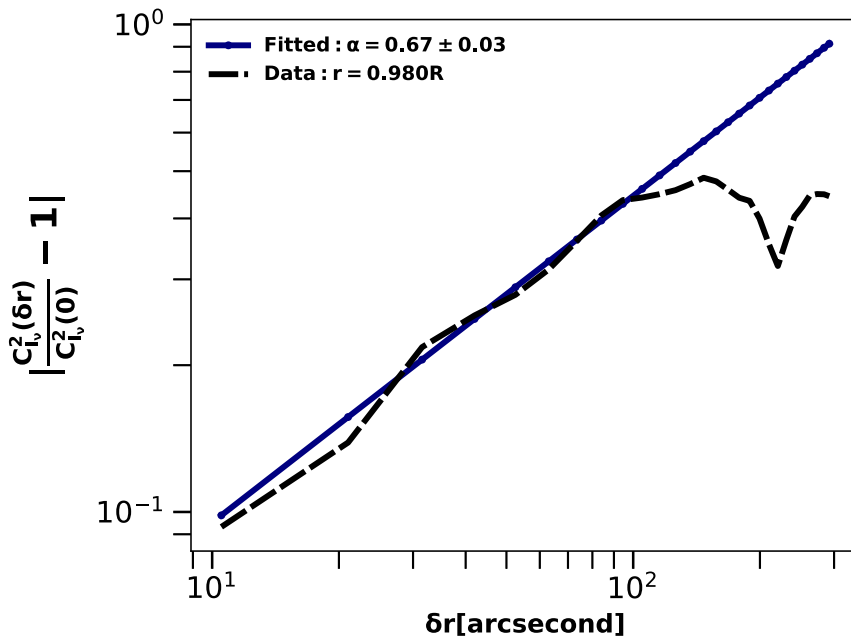


Fig. 3.5 : One of the best chosen spectra from region 3 (see figure 3.4).

Table 3.2 Fitted values of α for the spectra shown in figures 3.2 and 3.4.

radius(r/R)	α	radius(r/R)	α	radius(r/R)	α
0.613	0.64 ± 0.02	0.760	0.66 ± 0.03	0.980	0.67 ± 0.03
0.620	0.68 ± 0.03	0.767	0.68 ± 0.03	0.986	0.68 ± 0.03
0.627	0.67 ± 0.03	0.773	0.70 ± 0.03	0.993	0.70 ± 0.03
0.633	0.72 ± 0.04	0.780	0.69 ± 0.03	1.000	0.67 ± 0.03
0.640	0.70 ± 0.06	0.787	0.69 ± 0.03	1.007	0.70 ± 0.04
0.647	0.66 ± 0.07	0.793	0.67 ± 0.02	1.013	0.67 ± 0.04
0.653	0.63 ± 0.07	0.800	0.64 ± 0.02	1.020	0.64 ± 0.05

3.4 Results

In figure 3.2, we show the measured magnetic energy spectra of region 1 (0.613R-0.653R) and region 2 (0.670R-0.800R). The normalized statistics $|C_{I_v}^2(\delta r)/C_{I_v}^2(0) - 1|$ is shown on the y-axis while length scale δr (in unit of R) is shown on x-axis. Each panel of the figure 3.2, consists of seven magnetic energy spectrum based on the fitted power-law index being closest to the $2/3$ within its uncertainty measurement. To be compared easily, we have also plotted the $2/3$ law in each panel of figure 3.2. The proper discriminated spectra of this figure can be seen as figure A.1 in the appendix. The two best-fitted values of the spectra from region 1 and region 2 are shown in figure 3.3, along with their fitted α values as shown in the left corners. The two spectra in the figures are chosen such that they have the best reduced χ^2 and α closest to $2/3$. The x-axis of figure 3.3 is in the arcsecond unit. The spectra of region 3 are shown in figure 3.4, and it is plotted in the same way as figure 3.2. The proper discriminated spectra of this figure also can be seen in the appendix as figure A.2. The values of the fitted α for the regions 1, 2, and 3 with 1σ error bars are listed in the table 3.2. Figure 3.5 shows one of the seven spectra chosen from figure 3.4, which have the best fitted reduced χ^2 and α closest to $2/3$, than the others. The all investigated spectra at all radii i.e. from 0.524R-1.093R, are shown in the figures A.3 and A.4 in the appendix.

3.5 Discussion

Regions 1, 2 and 3 show the $\sim 2/3$ power-law behaviour for the correlation function $|C_{I_v}^2(\delta r)/C_{I_v}^2(0) - 1|$ and represents the trans-Alfvénic MHD nature as discussed in Goldreich and Sridhar (1995). The radial width of the regions 1, 2 and 3, which have statistics close to the $2/3$ power law, is $\sim 0.047R(7'')$. If we assume the distance of the Cassiopeia-A to be 2.5kpc, then this corresponds to the physical width of ~ 0.115 pc. Such magnetohydrodynamic turbulence corresponds to the trans-Alfvénic situation having the Alfvén Mach number $M_A = u_i/V_A = 1$. Here u_i is the injection velocity of the turbulence, and V_A is the Alfvén velocity. The dynamical evolution of the supernova remnants produces a contact discontinuity between the forward and reverse shocks in the SNRs (Laming, 2001). The position of the reverse shock in the SNR Cassiopeia-A is found to be at $0.760 \pm 0.040R$ ($114 \pm 6''$) (Arias et al., 2018), which is just in the vicinity of region 2 where $2/3$ power-law like statistics is found, so we call this region as a "reverse shock region" (or RSR in short). The reverse shock position in the X-ray frequency data is found to exist at $0.633 \pm 0.006R$ ($95 \pm 10''$) (Gotthelf et al., 2001), which again is in the proximity of region 1 where $2/3$ law holds up to some range of length scales. We will call region 1 as a subshock region (SSR in short). This difference in the radio reverse shock position and X-ray reverse shock position was noticed by the Arias et al. (2018) and they found that the reverse shock observed in the radio frequency observation is more centrally located (in respect to the expansion center of the SNR) than the observed in the x-ray frequency observation, and both were found to be coinciding at the western edge of the SNR. Our results show that, in the vicinity of the SSR, statistics of the spectrum have power-law, which only can happen if there exists a subshock at this position and not being observed in the radio frequency observation but produces the MHD condition favorable to those of the trans-Alfvénic nature. The reason behind calling region 1 as a subshock region is that the measured spectra at this radial position is not fully developed (see the upper panel of figure 3.2) as it

has cut off around 80", which seems to possess the property of a semi shock. The Gotthelf et al. (2001) noted that the radial position of the forward shock in the SNR Cassiopeia-A is at 1.020 ± 0.080 ($153 \pm 12''$), which is in the vicinity of the region 3, and this is the reason we will call it a forward shock region (FSR). Laming (2001) noted that a contact discontinuity exists between the forward and reverse shocks of the Cassiopeia A. From the above discussion, it is evident that found $2/3$ power-law-like statistics exist in the vicinity of the SNR Cassiopeia-A shocks, where Alfvén Match number M_A is expected to be close to 1. The explanation of the developed trans-Alfvénic MHD condition in the vicinity of the shocks exists in the magnetic field amplification at these radial positions, and it is discussed and summarised in a well-managed manner in Shimoda et al. (2018). Using the X-ray data observation, it now has been confirmed that in the SNR Cassiopeia-A, there exist magnetic field amplification (Berezhko and Völk, 2004). If we consider the shock speed ~ 2400 km/s as the injection velocity (at the longest scale) and the downstream amplified magnetic field, B_d of Cassiopeia-A $\sim 485 \mu\text{G}$ (Völk et al., 2005b); then the global value of M_A comes ~ 1.8 . Here we have considered the ambient density of the Cassiopeia-A to be 10^{-24}g/cm^3 (Badenes, 2010). Through the Doppler technique, the forward shock speed of the SNR Cassiopeia-A is measured to be 4000 ± 500 km/s (see Willingale), which gives the upper limit of the $M_A \sim 3.3$. These are the global estimates of the M_A , which show that they are very much close to the required value of 1 for the trans-Alfvénic MHD turbulence in the SNR. The precise estimates of M_A needs the exact values of the density, velocity, and magnetic field at the locations of SSR, RSR, and FSR. The results of the Shimoda et al. (2018) for the Tycho's SNR also show that the value of M_A would be ~ 1.8 in the Tycho's SNR, if the consideration of the shock speed ~ 5000 km/s (Williams et al., 2016) and the magnetic field $\sim 273 \mu\text{G}$ (Völk et al., 2005a) is taken for the Tycho's SNR. The spectra of these two SNRs (Tycho and Cassiopeia-A), along with their estimated global values of M_A , confirm that the MHD turbulence in these SNRs is of the trans-Alfvénic nature.

Found $2/3$ law in the SNR Cassiopeia-A at the radial position of the SSR predicts the existence of a subshock at this radial position. This represents that SNR Cassiopeia-A may also have a subshock in addition to the forward and reverse shocks. From the above conclusions, it is clear that in the radial window of around 0.115pc , the amplification of the magnetic field has taken place in the proximity of the noted shocks. The regions outside of these are not favorable to the trans-Alfvénic like MHD. The magnetic field amplification in the vicinity of SNR shocks most likely takes place because of the known instabilities, like Bell instability (Bell, 2004), acoustic instability (Drury and Falle, 1986) and RMI instability (Richtmyer, 1960; Sano et al., 2012). The exact mechanism of the magnetic field amplification or the instabilities can only be explained with the help of the very high-resolution interferometry and likely to be explained once SKA (Square Kilometer Array) becomes operational. The measured spectra at SSR have cutoff in its amplitude $\sim 80''$ and it is most likely the result of the developing stage of the trans-Alfvénic MHD; else there is also a possibility that beyond $\sim 80''$ there may be an interaction between the developed trans-Alfvénic MHD and above-mentioned instabilities. The measured spectra in our results (as well as the results from Tycho's SNR) show that their shape is of single power law in nature, as mentioned in Goldreich and Sridhar (1995). But to generalize this statement that SNR has the single power-law magnetic energy spectra, we need to measure the magnetic energy spectrum in more SNR similar to Cassiopeia-A and Tycho's. From our results, it is clear that these two young SNRs have the $2/3$ power-law statistics, and they should be capable of accelerating the CRs up to the knee energy with the shock compression ratio models as discussed in Parizot et al. (2006). However, the observational results have shown that Cassiopeia-A is only a TeV candidate and can not accelerate CR protons up to the knee energy (Zhang and Liu, 2019).

To summarize, the magnetic energy spectrum in the proximity of the young SNRs Cassiopeia-A and Tycho shocks are of trans-Alfvénic nature (Kolmogorov like). The

supernova remnants Cassiopeia-A may have a subshock at the radial location of 95" in addition to their known forward and reverse shocks.